

## Saturation Mechanism for a Storage-Ring Free-Electron Laser

Michel Billardon,<sup>(a)</sup> David Garzella,<sup>(b)</sup> and Marie Emmanuelle Couprie<sup>(b)</sup>

*Laboratoire pour l'Utilisation du Rayonnement Electromagnetique,  
Centre National de la Recherche Scientifique-Commissariat à l'Energie Atomique-Ministère de l'Education Nationale,  
Bâtiment 209D, Université de Paris-Sud, 91405 Orsay CEDEX, France*  
(Received 24 August 1992)

Equilibrium and dynamical properties of a storage-ring free-electron laser are shown as resulting from the combined effects of two different saturation mechanisms. The first one is the laser-induced energy spread of the electron beam. The second mechanism is due to an imperfect longitudinal synchronism between the electron and laser pulses. Consequences are briefly described.

PACS numbers: 41.60.Cr

During the last years, several experiments were devoted to the free-electron laser (FEL) working with an electron or positron storage ring (SRFEL) [1-5]: ACO and Super-ACO at Orsay, VEPP3 at Novosibirsk, and TERAS and UVSOR in Japan. Their main goal is to provide a short-wavelength tunable laser. However, several difficulties appear: The interaction between the laser light and the electrons leads to a cumulative perturbation for the stored beam since the same electrons are used at each pass. The beam properties are mainly defined by the optical gain evolution due to the laser saturation mechanism, which results in a more or less stable laser after some transient regimes. For an SRFEL, the classical theory [6] implies mainly a saturation mechanism through a laser-induced energy spread for the electron distribution: For a particular electron with a given energy, the laser interaction can lead to an enhancement (absorption process) or to a diminution (optical gain process) of the electron energy. For an electron bunch ( $10^{10}$  electrons), both processes are simultaneously present, with the laser operation resulting from a dominant optical gain process. However, the laser intensity induces an enhancement of the energy spread with respect to the initial one and then a gain diminution, since a lower number of electrons corresponds to the resonant condition. An equilibrium situation is obtained for the peak value of the electron distribution where the classical threshold condition (saturated gain equal to losses) is respected. In this Letter we show that such a simple mechanism cannot explain all the properties of the FEL, and that experimental and theoretical features lead to the conclusion that another saturation mechanism must be involved, with the FEL properties resulting from the combination of both mechanisms.

Storage-ring FELs operate with a particular kind of undulator, an optical klystron, and the optical gain is determined by the formula

$$g_0 \propto [(N + N_d)/\sigma] \exp[-8\pi^2(N + N_d)^2\sigma_\gamma^2], \quad (1)$$

where  $\sigma_\gamma$  is the relative rms energy spread,  $\sigma$  is the corresponding bunch length, and  $N + N_d$  is the interference order of the optical klystron. For Super-ACO the optimum values are  $N + N_d \cong 100$  for  $\sigma_\gamma = 8 \times 10^{-4}$ . On Super-

ACO several threshold experiments show that an initial optical gain of around 2.5% per pass exists, which corresponds to the expected value. With the losses being of the order of 0.5%, saturation mechanisms must explain a gain reduction by a factor of 4 or 5 in order to respect the equilibrium condition. Different experiments conducted on Super-ACO show that such a reduction cannot be explained with the classical theory taking into account only the energy spread.

First of all, the positron bunch length was measured with a "dissector" (picosecond detector based on a stroboscopic electro-optical method [7,8]) for laser-off and laser-on conditions. From Eq. (1) the experimental values lead to a maximum gain reduction of the order of 50%, inconsistent with the factor of 4 necessary to explain the equilibrium condition. The second experimental test results from a study of the laser rise time: Starting from a laser-off situation, when the gain is suppressed in order to obtain a complete relaxation of the positron beam and then the maximum possible gain ( $Q$ -switched laser), the laser intensity grows exponentially when the gain is reestablished, in accord with the saturation mechanism. For an optical gain of 2.5% and losses of 0.5%, a rise time of 12  $\mu$ s must be expected during the exponential growth. Experimentally we observe a rise time of at least 50  $\mu$ s and more generally 80  $\mu$ s, whatever the experimental conditions (ring current ranging from 4 to 60 mA,  $N + N_d = 10$  to 100, etc.). These values disagree completely with the classical theory.

In consequence, one can conclude from the previous phenomena and from the laser micropulse structure, as explained below, that a second possible saturation mechanism, resulting from the "tuning," must be considered. The laser interaction is due to the longitudinal overlap between the electron pulse circulating in the storage ring and the optical pulse circulating in the optical cavity. For a perfect synchronism, and then a maximum optical gain, both periods must be equal. A small detuning (difference between the periods) leads to a cumulative delay between the electron and laser pulses, and reduces the longitudinal overlap and the optical gain. Such a situation can be modeled with the pass-to-pass longitudinal evolution:

$$y_{n+1}(\tau) = R^2 y_n(\tau - \varepsilon) [1 + g(\tau)] + i_s(\tau), \quad (2)$$

where  $y_n(\tau)$  is the longitudinal profile of the laser pulse,  $\tau$  is the longitudinal coordinate inside the micropulse, the origin being the synchronous electron,  $g(\tau) = g_0 \times \exp[-(\tau^2/2\sigma^2)]$  is the longitudinal profile of the optical gain proportional to the electron density,  $R^2$  is the mirror reflectivity,  $i_s$  is the spontaneous emission also proportional to the electron density profile, and  $\epsilon$  is the detuning per pass for the laser micropulse with respect to the electron bunch. In the absence of energy spread,  $g(\tau)$  is time independent. Numerical simulations with Eq. (2) show that, except for the case  $\epsilon \equiv 0$ , an equilibrium situation is obtained where the longitudinal profile  $y(\tau)$  does not evolve and has a maximum value for a position  $\tau_m$  close to the value corresponding to the threshold condition  $g(\tau_m) = \text{losses}$ , even for a small  $\epsilon$  value. Finally, a simple detuning determines a saturation process, except for the case of a perfect tuning  $\epsilon \equiv 0$  where the laser intensity has an exponential divergence.

An actual laser saturation mechanism results from this "detuning process," combined with the classical energy-spread process [6], where the profile  $g(\tau)$  is perturbed by the laser interaction. The laser-induced energy spread is defined by the normalized parameter  $\Sigma = (\sigma_\gamma^2 - \sigma_0^2) / (\sigma_e^2 - \sigma_0^2)$  ( $\sigma_0$  is the laser-off energy spread and  $\sigma_e$  is the laser equilibrium value for a perfect tuning), whose evolution is given by the formula [9]

$$\frac{d\Sigma}{dt} = \frac{2}{\tau_s} (I - \Sigma), \tag{3}$$

where  $I$  is a normalized laser intensity,

$$I(t) = \int_{-\infty}^{+\infty} y(t, \tau) d\tau \tag{4}$$

( $\Sigma = I \cong 1$  corresponds to the equilibrium for a perfect tuning). For an optical klystron the gain is extremely sensitive to the energy spread. We can neglect the variation of the bunch length  $\sigma$ , so that from (1) the peak gain evolves as

$$g_0 = g_i (P/g_i)^\Sigma, \tag{5}$$

where  $g_i$  is the initial gain without laser interaction and  $P$  is the cavity losses. The coupled equations (1)–(5) were used in order to simulate the behavior of a laser submitted simultaneously to a detuning and to the energy spread. Generally speaking, these equations lead to a complicated nonlinear second-order system for temporal evolution of each variable [longitudinal profile  $y(\tau)$ , laser intensity  $I(\tau)$ , energy spread  $\Sigma(\tau)$ ], the solution having or not having an oscillating behavior. Numerical simulations for various conditions give results in excellent agreement with the experimental results. Only some of them are detailed in this paper.

The best way to determine the dynamics of this system is by a  $Q$ -switched experiment where the gain is first completely suppressed (in order to eliminate the previous laser intensity) and then rapidly reestablished. Figure 1 presents the experimental results obtained with Super-

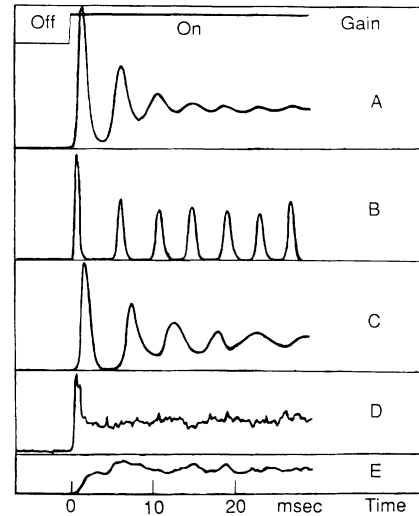


FIG. 1. Laser intensity transient regimes measured on Super-ACO for different values of the longitudinal detuning  $\Delta T/T$ . (a) Perfect synchronism. (b)  $\Delta T/T = 2 \times 10^{-7}$ . (c)–(e) Higher values of the detuning (maximum  $\Delta T/T = 2 \times 10^{-6}$ ).

ACO for different conditions of detuning. Generally, the transient response is an exponential growth of the laser intensity, leading to a first intense macropulse when the saturation mechanism occurs, followed by some relaxation oscillations more or less damped, and finally a stable regime. For perfect synchronism [Fig. 1(a)] the relaxation oscillations are rapidly damped by the synchrotron damping time  $\tau_s$ , and the permanent regime is a cw laser. For a small detuning [Fig. 1(b)] there are no relaxation oscillations and one obtains a stable pulsed laser immediately after the first macropulse. For a larger detuning [Fig. 1(c)] one again finds the same behavior as for perfect synchronism. Finally for very large detuning [Figs. 1(d) and 1(e)] there are no longer relaxation oscillations; the system is completely damped so that the exponential growth leads immediately to a cw laser.

Simulations made with Eqs. (1)–(5) exhibit exactly the same behavior. For the long-time regime, Fig. 2 presents the calculated damping time of the relaxation oscillations versus the detuning; a small detuning corresponds to an enhancement of this damping time, reaching several orders of magnitude in a short range of detuning: In this region a stable pulsed laser is obtained and no attenuation of these oscillations was detected, even after  $10^5$  passes; simultaneously all the other parameters (micropulse position and width, peak power, integrated power) oscillate with the same period. For a larger detuning the damping time decreases (cw laser as the permanent regime) and reaches practically the zero level when the relaxation oscillations disappear. The calculated energy spread decreases simultaneously with the detuning, and the position of the laser micropulse is displaced with respect to the center of the electronic distri-

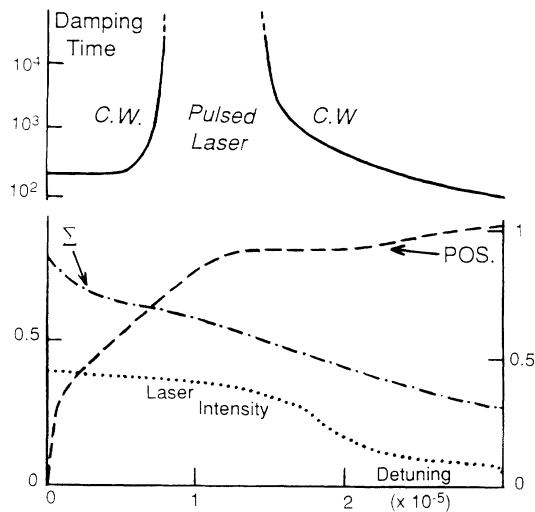


FIG. 2. Evolution with the detuning of the main laser parameters calculated from the theoretical model. For the simulation,  $g_0=60\%$  and  $\tau_s=25 \mu s$  were chosen in order to reduce the calculation time. The damping time is evaluated in units of number of passes. The position (POS) of the laser micropulse with respect to the center of the electronic density is evaluated as a fractional part of the bunch length  $\sigma$ .

bution, as shown in Fig. 2. Such a sensitivity of the damping time to a small detuning explains why a pulsed FEL is generally obtained. The stable cw laser obtained on Super-ACO is due to the exceptional stability of the storage ring. These simulations also explain why the measured energy spread is lower than the expected one, the calculated laser-induced energy spread  $\Sigma$  being extremely sensitive to the detuning.

The second interesting feature is the laser rise time during the initial exponential growth. Figure 3 presents the temporal evolution of the main parameters for this region, resulting from a simulation for the Super-ACO conditions and for two values of detuning. The energy spread  $\Sigma$  is negligible during this process, but the position of the laser micropulse evolves very quickly [Fig. 3(b)]. Figure 3(c) presents the evolution of the laser intensity, which is roughly an exponential growth but with a rise time around  $30 \mu s$ , higher than the expected one for a perfect tuning ( $\tau=12 \mu s$ ); this calculated value is in good agreement with the measured one. These results illustrate the sensitive dependence of the exponential growth to a small detuning.

The validity of the model was also tested with the experimental determination of the laser micropulse structure made with a "dissector" [7,8]. Figure 4 presents the superposition of the laser micropulse and of the electron distribution measured with the spontaneous emission from the undulator. Pulses B and C correspond to the case of a large positive and negative detuning. Schematically, in this case the position of the laser pulse corresponds roughly to an electronic density where  $g(\tau)$

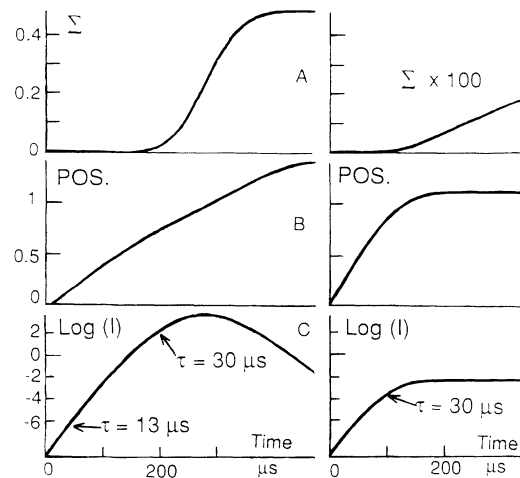


FIG. 3. Temporal evolution of the main parameters during the first step of the transient regime, calculated for the Super-ACO case. Left side: detuning  $\Delta T/T=1 \times 10^{-6}$ . Right side:  $\Delta T/T=2 \times 10^{-6}$ .

$\cong$  losses, showing that saturation depends mainly on the detuning, with the energy spread being highly reduced. This feature is in agreement with the results of the simulation (right side of Fig. 3) where the laser micropulse position varies very quickly with the detuning. Pulses A in Fig. 4 correspond to "perfect" synchronism. It can be viewed that successive micropulses recorded during 0.2 s evolve rapidly in position. In spite of the good stability of the storage ring on a long time scale, there are probably some residual high-frequency fluctuations corresponding to a small detuning or a perturbation of the shape of the electron beam, so that, even if the laser macrotemporal structure is stable, there are some fluctuations of the laser microtemporal structure. Actually, a perfect synchronism can be maintained only during a very short time (less than 1 s) and generally we observe a fluctuating micropulse as illustrated in Fig. 4, traces A.

All these results illustrate that general features of a storage-ring FEL are highly dependent on a small detun-

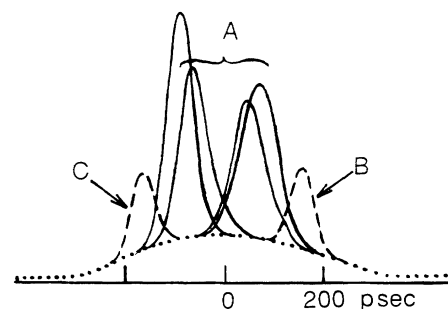


FIG. 4. Microtemporal structure of the laser measured on Super-ACO.  $\cdots$ : longitudinal profile of the electron bunch. Laser profile: "perfect synchronism" (A), maximum positive and negative detuning  $\Delta T/T \cong 2 \times 10^{-6}$  (B and C).

ing. The classical saturation mechanism due to the energy spread is dominant only for a very small detuning or for a laser very close to the threshold condition. Even for a particularly stable storage ring such as Super-ACO, residual fluctuating detunings (or equivalent fluctuations of the shape of the longitudinal electron beam profile) determine the main saturation process. The consequence is a more complicated theory taking into account both saturation processes, with, probably, a rapidly fluctuating situation for the tuning, so that predictions based only on a perfect tuning are unreliable. Illustrations of such a situation are the peak power for a  $Q$ -switched laser reduced by 1 order of magnitude with respect to the expected one, the possibility of a naturally permanent pulsed laser (even in the absence of noise or gain modulation), and the high-frequency instabilities of the micropulse structure. Other possible consequences to be reconsidered are those for the expected average laser power (Renieri limit), the estimated gain value, secondary laser parameters (temporal width, spectral width, etc.), and the chaos mechanism [10]. We believe that these consequences must be considered for the design of future storage-ring FELs.

This work was supported by Direction des Recherches, Etudes et Techniques (Contract No. 89/165).

---

<sup>(a)</sup>Permanent address: Laboratoire Optique Physique, Ecole

Supérieure de Physique et de Chimie Industrielles, 10 rue Vauquelin, 75231 Paris CEDEX 05, France.

- <sup>(b)</sup>Permanent address: Commissariat à l'Énergie Atomique, Service Photons, Atomes et Molécules Centre d'Études Nucleaires Saclay, 91191 Gif-sur-Yvette, France.
- [1] M. Billardon, P. Elleaume, J. M. Ortega, C. Bazin, M. Bergher, M. Velghe, D. A. G. Deacon, and Y. Petroff, *Phys. Rev. Lett.* **51**, 1652 (1983).
  - [2] M. E. Couprie, M. Billardon, M. Velghe, C. Bazin, J. M. Ortega, R. Prazeres, and Y. Petroff, *Nucl. Instrum. Methods Phys. Res., Sect. A* **296**, 13 (1990).
  - [3] I. B. Drobyazko, G. W. Kulipanov, V. N. Litvinenko, I. V. Pinayev, V. M. Popik, I. G. Silvestrov, A. N. Skrinsky, A. S. Sokolov, and N. A. Vinokurov, in *Free Electron Lasers II*, edited by Y. Petroff, SPIE Proceedings Vol. 1133 (SPIE—International Society for Optical Engineering, Bellingham, WA, 1989), p. 2.
  - [4] T. Yamazaki, K. Yamada, S. Sugiyama, H. Ohgaki, T. Tomimasu, T. Noguchi, T. Mikado, M. Chiwaki, and R. Suzuki, *Nucl. Instrum. Methods Phys. Res., Sect. A* **309**, 343 (1991).
  - [5] S. Takano, H. Hama, and G. Isoyama, *UVSOR Activity Report 1991* (UVSOR, Okazaki, Japan, 1991).
  - [6] P. Elleaume, *J. Phys. (Paris), Colloq.* **44**, C1-333 (1983).
  - [7] E. I. Zinine, *Nucl. Instrum. Methods Phys. Res., Sect. A* **208**, 439 (1983).
  - [8] M. E. Couprie, V. M. Popik, E. I. Zinine, A. Delboubé, D. Garzella, M. Velghe, and M. Billardon, *Nucl. Instrum. Methods Phys. Res., Sect. A* **318**, 59 (1992).
  - [9] P. Elleaume, *J. Phys. (Paris)* **45**, 997 (1984).
  - [10] M. Billardon, *Phys. Rev. Lett.* **65**, 713 (1990).